Energy Reports 8 (2022) 4512–4524

Contents lists available at ScienceDirect

Energy Reports

journal homepage: www.elsevier.com/locate/egyr

Research paper

Multi-objective optimal scheduling of microgrid with electric vehicles

Yu Mei [a,b], Bin Li [a], Honglei Wang [a,c,*], Xiaolin Wang [d], Michael Negnevitsky [d]

[a] Electrical Engineering College, Guizhou University, Guiyang 550025, China
[b] School of Computer and Information, Qiannan Normal University for Nationalities, Duyun 558000, China
[c] Key Laboratory of "Internet+" Collaborative Intelligent Manufacturing in Guizhou Provence, Guiyang Guizhou 550025, China
[d] School of Engineering, University of Tasmania, Hobart, TAS, 7005, Australia

ARTICLE INFO

Article history:
Received 21 November 2021
Received in revised form 21 February 2022
Accepted 15 March 2022
Available online xxxx

Keywords:
Microgrid
Electric vehicles
Multi-objective optimization
Two-person zero-sum game
Adaptive simulated annealing particle swarm optimization algorithm

ABSTRACT

With the increasing global attention to environmental protection, microgrids with efficient usage of renewable energy have been widely developed. Currently, the intermittent nature of renewable energy and the uncertainty of its demand affect the stable operation of a microgrid. Additionally, electric vehicles (EVs), as an impact load, could severely affect the safe dispatch of the microgrid. To solve these problems, a multi-objective optimization model was established based on the economy and the environmental protection of a microgrid including EVs. The linear weighting method based on two-person zero-sum game was used to coordinate the full consumption of renewable energy with the full bearing of load, and balance the two objectives better. Moreover, the adaptive simulated annealing particle swarm optimization algorithm (ASAPSO) was used to solve the multi-objective optimization model, and obtain the optimal solution in the unit. The simulation results showed that the multi-objective weight method could diminish the influence of uncertainty factors, promoting the full absorption of renewable energy and full load-bearing. Additionally, the orderly charging and discharging mode of EVs could reduce the operation cost and environmental protection cost of the microgrid. Therefore, the improved optimization algorithm was capable of improving the economy and environmental protection of the microgrid.

1. Introduction

With the increase in global demand for electricity, problems regarding energy and the environment have become important social problems worldwide. Fossil fuel combustion in traditional thermal power plants has caused severe environmental pollution, and the traditional power grid has the disadvantages of high cost and low efficiency. Therefore, electric vehicles (EVs) that support clean energy by utilizing renewable energy to generate electricity have been favoured all over the world. A microgrid is a small power generation and distribution system involving renewable energy and energy storage devices. It plays an important role in power systems on account of its strong security, high utilization rate of renewable energy, and low operation cost (Tabar et al., 2017). However, the intermittence and fluctuation of renewable energy and the uncertainty in demand pose great challenges to the supply and demand balance of the microgrid, and the safe and economic dispatching of the system. Due to the development of EVs, they can be added to microgrid scheduling as an important distributed power supply. Therefore, an increasing number of scholars have begun studying the optimal scheduling of the microgrid including EVs.

EVs can be regarded as mobile energy storage device participating in the operation of the microgrid, that could become the impact load on the demand side. If it is not managed, the EVs will charge disorderly, leading to the superposition of peak load. When V2G (Vehicle to grid) technology is used to guide it to participate in the dispatching of the microgrid, it is regarded as the supply side, which not only reduces the uncertainty of renewable energy, and but also meets the load demand of the microgrid. With the increase in the access rate of EVs, it is necessary to formulate a dispatch plan to reduce the operating cost of a microgrid system including EVs. Sedighizadeh et al. (2020) considered EVs in dispatching and found that the corresponding operation cost was reduced. Jiang et al. (2019) studied the economic scheduling process of the microgrid under ordered and disordered modes of large-scale EVs, and the results showed that the ordered charge–discharge mode could effectively reduce costs in the microgrid. Hui et al. (2020) analysed the orderly charging and discharging, and random charging of EVs to study the impact of the charging and discharging behaviours of EVs on microgrid scheduling, and the results showed that the charging and discharging behaviours

* Corresponding author at: Electrical Engineering College, Guizhou University, Guiyang 550025, China.
E-mail addresses: 1957429992@qq.com (Y. Mei), binli943@163.com (B. Li), hlwang@gzu.edu.cn (H. Wang), xiaolin.wang@utas.edu.au (X. Wang), michael.negnevitsky@utas.edu.au (M. Negnevitsky).

https://doi.org/10.1016/j.egyr.2022.03.131

of EVs could effectively improve the economy of the microgrid and reduce environmental pollution. From the aforementioned literature, it is seen that the orderly dispatching of EVs is of great significance for reducing the cost of the microgrid and improving its environmental benefits.

In previous research of microgrid dispatching, most scholars often considered multiple objective functions to optimize the dispatching results. Commonly used multi-objective functions include the generation cost and environmental cost of the microgrid (Alomoush, 2019), full life cycle cost and wind abandonment rate (Ding et al., 2020), operation cost and reliability (Chamandoust et al., 2020). For a grid connected microgrid, the reliability of microgrid operation has been greatly improved by the support of the distribution network. However, the energy of a distribution network is mainly generated from fossil energy, which cause serious pollution to the environment. Thus, microgrids consist of renewable energy and fuel devices. Although the addition of renewable energy reduces the usage of fuel and improves the environmental protection of the microgrid, the cost of these renewable energy devices is high. Hence, to make the microgrid economic and environmental friendly, economy and environmental protection are the main objective functions. Geng et al. (2021) and Meng et al. (2018b) solved the day-ahead scheduling plan by combining the generation cost and environmental cost of microgrid operation. The optimal unit output obtained not only improved the environmental protection of the system, but also the utilization rate of renewable energy. Li and Xia (2019) and Shayeghi and Shahryari (2017) considered the optimal total cost of the system and the lowest pollution gas emission as the objective functions, and the scheduling results showed that a scheduling plan considering the economy and environmental protection yielded better comprehensive benefits for the supply side, demand side, and natural environment simultaneously. From the aforementioned literature, it is seen that for the supply side and the demand side, a dispatching plan considering the economy reduces the power generation cost of the microgrid, and the electricity consumption cost of the consumers. For the natural environment, a dispatching plan considering environmental protection is more beneficial for the environment. Therefore, considering both economy and environmental protection is of great practical significance to the scheduling plan of a microgrid.

There are two main methods for solving multi-objective optimization problems. One method involves solving the Pareto solution set using a multi-objective optimization algorithm, and selecting the optimal solution similar to the ideal solution, through prioritization technology (He et al., 2019; Mehrabadi and Sathiakumar, 2020; Zheng et al., 2020). Liu et al. (2019) targeted the user's comfort level, operation cost, and environmental protection cost, and used the non-dominated sorting genetic algorithm II (NSGA-II) to obtain the Pareto solution set; the analytic hierarchy process (AHP) was used to obtain the optimal solution from all the Pareto solutions, but its subjectivity was too strong. Javidsharifi et al. (2018) proposed an intelligent evolutionary multi-objective improved bird-mating optimization algorithm, to solve the multi-objective optimization problems of environment and economy. The Pareto solution set was obtained, and the method of obtaining the optimal solution from all Pareto solutions was given. This multi-objective optimization algorithm could avoid adjusting the weight of each goal, and directly solve all the Pareto solutions. However, it could not provide a unique optimal solution for the decision-maker. Therefore, multi-objective decision-making technology was required to overcome this defect. The second method for solving multi-objective optimization problems includes weighing the multiple objectives (Elattar, 2018; Meng et al., 2018a), so as to convert the multi-objective optimization problem into a single objective optimization problem. Lu et al. (2018) converted the three optimization objectives of system operation cost, environmental cost, and load change into one optimization objective by adopting the linear weighting method and analysed the scheduling results selected with different weights. The results showed that operators could use cost weight factors to control the scheduling results. To ensure the more economical and environmentally friendly operation of the microgrid, and fully utilize the advantages of distributed generation, Huang et al. (2019) proposed the two objective functions of minimum system operation cost and minimum environmental cost, which were transformed into a single objective using the linear weighting method, and their weights were determined by the preference of decision-makers. In the aforementioned studies, although the linear weighting method was used to transform the multi-objective optimization problem into a single-objective optimization problem, and finally provide the decision maker with a unique solution, the weight setting among multiple objectives poses a huge challenge to the decision maker.

When using the linear weighting method to coordinate multiple optimization objectives, the weights of different objectives represent the importance of each objective, and have a significant impact on the scheduling results. Currently, the commonly used weight determination methods include AHP (Li et al., 2015), the dualistic factor contrast method (Yang et al., 2018b) and expert scoring method (Wang et al., 2019). However, these methods have the disadvantage of strong subjectivity, and are influenced by uncertain factors acting on the system scheduling results. Yu et al. (2019) established an optimal dispatching model of a power system which comprehensively considered the power grid purchase cost and power generation coal consumption, and introduced the zero-sum game idea to resolve the dispatching model, which solved the subjective problem of multi-objective weight selection. Xu et al. (2016) proposed a multi-objective optimization method based on the two-person zero-sum game weight coefficient method, for a grid-connected composite energy storage microgrid including photovoltaics, liquid flow batteries and lithium batteries, to maximize the utilization of renewable energy and minimize the impact of grid-connected operation of the microgrid. Therefore, it was seen that the two-person zero-sum game could solve the problem of multi-objective weight selection in the micro-grid energy dispatching strategy, and could reduce the influence of uncertain factors.

An intelligent optimization algorithm can effectively solve most optimization problems. Intelligent optimization algorithms have been widely used in the scheduling of the microgrid. Ebrahim et al. (2020), Monteiro et al. (2020), Moradi et al. (2015) and Vivek et al. (2017) used the particle swarm optimization (PSO) algorithm to solve several optimization problems related to the microgrid. The PSO algorithm has fast convergence speed; however, because all particles fly in the direction of the optimal solution during convergence, the particles tend to become identical and lose their diversity, which makes the algorithm fall into the local optimum easily and thus do not yield the global optimal solution (Chen et al., 2013). The weight in the particle swarm was improved to balance the convergence speed and optimization ability of the PSO algorithm (Xue et al., 2019). Furthermore, Lu et al. (2017) improved the inertia weight and learning factor of the PSO algorithm and used it to solve the optimization model. Jeong et al. (2010) proposed a novel binary PSO algorithm based on quantum computing, named quantum particle swarm optimization algorithm, which improved the convergence and stability of the algorithm, but it still possessed the defect of falling into the local optimal solution. Additionally, Zhao et al. (2020b) used differential evolution to introduce quantum PSO, used the improved algorithm to solve the problem, has and yielded better performance. Currently, the improved PSO algorithms do not effectively solve the problem of easily falling into

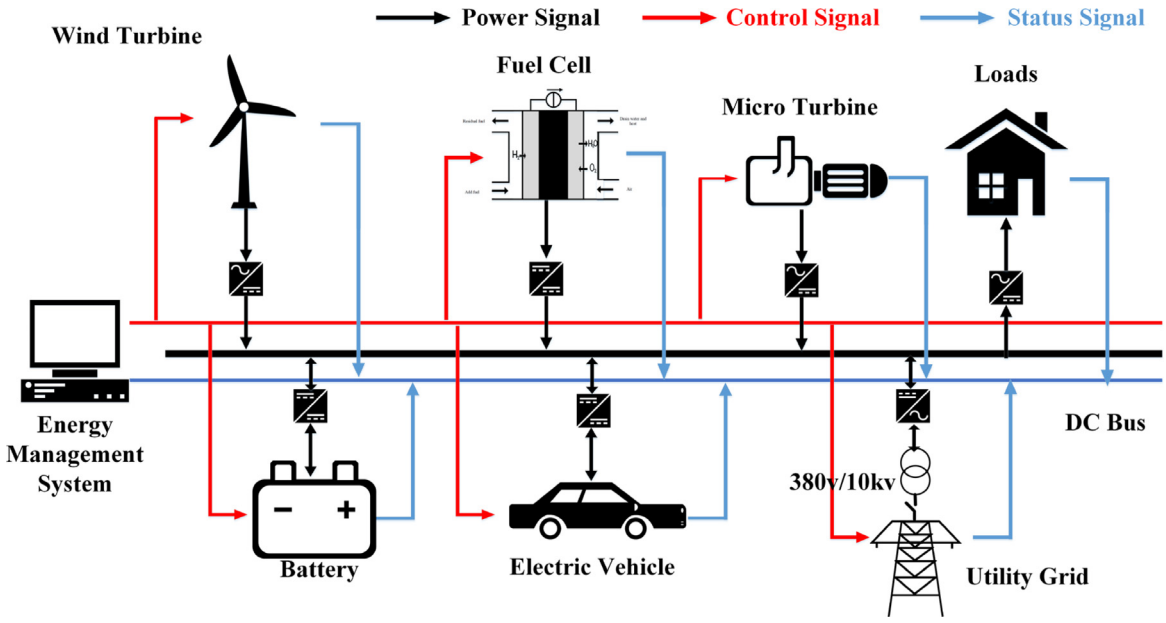

Fig. 1. The structure of microgrid.

the local optimum, thus, further improvement of the algorithm is of great significance.

Therefore, to realize full consumption of renewable energy and full load-bearing, and improve the efficiency of the microgrid, a microgrid system including the power of EVs was established in this paper. Currently, the main direction of microgrid optimization dispatching is economy and environmental protection. To improve the benefits of the microgrid, the operating cost and environmental maintenance of the microgrid were selected as objective functions in this paper. Furthermore, to achieve a more objective balance among multiple objectives, and provide a unique solution for decision-makers, we used the linear weighting method based on the two-person zero-sum game, for transforming the multi-objective optimization problem into a single-objective optimization problem. Additionally, we proposed the adaptive simulated annealing particle swarm optimization algorithm (ASAPSO), and the adaptive weight and optimization mechanism of simulated annealing were used to improve the PSO algorithm, to prevent the algorithm from falling into a local optimal solution, and obtain the optimal scheduling plan.

In summary, the main contributions of this work in comparison to existing literature include the following:

- A microgrid system with a five-port output of EVs was established. The disordered charging of EVs was analysed, and the real-time electricity price was used to guide the orderly charging and discharging of EVs, to realize peak load reduction and valley filling in the microgrid.
- In the determination of multi-objective weights, the two-person zero-sum game was used to consider the economy and environmental protection of the microgrid, which made the selection of weights more objective, reduced the interference of uncertain factors, and reduced the purchase of electricity from the distribution network.
- To improve the optimization ability of the algorithm and obtain a global optimal solution, the PSO algorithm was improved, and ASAPSO was used to optimize the scheduling strategy of the microgrid.

The remainder of this paper is organized as follows. The microgrid system model is presented in Section 2. In Section 3, the multi-objective scheduling system, the actual constraints, and the charging and discharging strategies of EVs are introduced. ASAPSO is proposed in Section 4. In Section 5, we introduce the optimization model of microgrid dispatching. Finally, the conclusion of the work is presented in Section 6.

2. Model of the microgrid

The microgrid studied in this paper, included wind turbine (WT), battery (BT), fuel cell (FC), micro gas turbine (MT), and EVs. The models of the WT, BT, FC, and MT were referenced from Lu et al. (2017) and Yang et al. (2018a). Fig. 1 shows the structure of the microgrid.

In this study, we assumed that the driving habits of electric car users were identical to those of traditional petrol-powered car users. The last round-trip time of EVs was obtained using normal distribution approximation (Hui et al., 2020), and according to Lu et al. (2018), the probability density function of starting charging time was set to 24 scheduling periods. 96 scheduling periods were adopted in this paper, the travel time was $t_0 \sim N\left(\mu_t, \delta_t^2\right)$, and its probability density function was expressed as follows:

$$f_1(t) = \begin{cases} \dfrac{4}{\sqrt{2\pi}\sigma_1} e^{-\frac{(t+96-\mu_1)^2}{2\sigma_1^2}} & 0 \le t \le \mu_1 - 48 \\ \dfrac{4}{\sqrt{2\pi}\sigma_1} e^{-\frac{(t-\mu_1)^2}{2\sigma_1^2}} & \mu_1 - 48 < t \le 96 \end{cases} \tag{1}$$

where $\mu_1 = 70.4$ is the expectation at the beginning of charging of EVs, and $\sigma_1 = 3.40$ is the standard deviation of the charging time of EVs.

The mileage, S of EVs obeyed lognormal distribution, that is, $S \sim \log N\left(\mu_s, \delta_s^2\right)$, and its probability density function was expressed as follows:

$$f_s(x) = \frac{1}{x}\frac{1}{\delta_s\sqrt{2\pi}} \exp\left(-\frac{(\ln x - \mu_s)^2}{2\delta_s^2}\right) \tag{2}$$

where $\mu_s = 3.20$ is the expected daily mileage of EVs, and $\sigma_1 = 0.88$ is the standard deviation of the daily mileage of EVs.

3. Multi-objective scheduling system

3.1. Objective function

In this paper, the microgrid system operated in the grid-connected mode. Under the consideration of the economy and environmental protection of the microgrid, a multi-objective economic dispatch model with the goal of minimizing the operating cost and environmental protection cost of the microgrid was established.

3.1.1. Objective function 1: Operation cost of microgrid is minimum

C_1 is the operation cost of the microgrid, which includes the fuel cost of MT and FC, the operation and maintenance cost, and depreciation cost of each power supply device, the interaction cost between the microgrid and the distribution network, and the electricity purchase cost of the microgrid from EVs. Therefore, it was expressed as follows:

$$C_1 = C_{fuel} + C_{om} + C_{dp} + C_{grid} + aC_{ev} \tag{3}$$

When EVs are connected to the microgrid disorderly, $a = 0$. When EVs are connected to the microgrid orderly, $a = 1$.

The fuel cost is mainly generated from MT and FC. Therefore, fuel cost of the microgrid was described as follows:

$$C_{fuel} = C_{MT} + C_{FC} \tag{4}$$

where C_{MT}, C_{FC} are the fuel costs of MT and FC, respectively.

In the operation process of distributed power generation, it is necessary to check and maintain regularly to ensure the stable and reliable operation of distributed power generation equipment. Therefore, its operating cost, C_{om} and maintenance cost, C_{dp} were described as follows:

$$C_{om} = \sum_{t=1}^{T}\sum_{i=1}^{N} K_{om,i}P_i(t)\Delta t \tag{5}$$

$$C_{dp} = \sum_{T=1}^{T}\sum_{i=1}^{N} \frac{ADCC_i}{P_{cci} \times 8760 \times k_i} P_i(t)\Delta t \tag{6}$$

$$ADCC_i = c_{\cos t,i}\frac{r_i(1+r_i)^{l_i}}{(1+r_i)^{l_i}-1} \tag{7}$$

where $K_{om,i}$, $ADCC_i$, $c_{\cos t,i}$, r_i, k_i, l_i, and P_{cci} are the operation and maintenance coefficient, annual depreciation cost, initial installation cost, capacity factor, annual depreciation cost, depreciation life, and rated power of type i distributed generation, respectively, and $P_i(t)$ is the output power at t.

Microgrids can guide the users' electricity consumption behaviour through electricity prices to ensure that it operates in a more economically. This was expressed as follows:

$$C_{grid} = \sum_{t=1}^{T}(c_{buy}(t)P_{buy}(t) - c_{sell}(t)P_{sell}(t))\Delta t \tag{8}$$

where $c_{buy}(t)$ and $c_{sell}(t)$ are the prices of electricity purchase and sale, at time t, respectively; $P_{buy}(t)$ and $P_{sell}(t)$ are the powers purchased and sold, at time t, respectively.

If the EVs must be connected to the microgrid orderly, to minimize its own cost, the owner will charge it as much as possible when the electricity price is low under the influence of real-time electricity price, and sell electricity to the microgrid when the electricity price is high, such that "cutting peak and filling valley" is achieved (Zhao et al., 2020a). From the user side, the charge and discharge costs of EVs include the charging cost and power sales revenue of EVs. From the microgrid, the power purchase cost of microgrid to EVs includes the power purchase expenditure and power sales revenue of the microgrid to EVs. The cost of purchasing electricity from EVs by microgrid was expressed as follows:

$$C_{ev} = \sum_{t=1}^{T} C_p(t)\,|P_{ev}(t)|\,\Delta t \tag{9}$$

where $C_p(t)$ and $P_{ev}(t)$ are the electricity purchase price and electricity purchase power of EVs from the microgrid at time t, respectively. When $C_p(t) > 0$, the microgrid purchases electricity from the EVs; when $C_p(t) < 0$, the microgrid sells electricity to the EV; when $P_{ev}(t) > 0$, the EV is charged; when $P_{ev}(t) < 0$, the EV is discharged.

3.1.2. Objective function 2: Environmental protection cost of microgrid is minimum

C_2 is the cost of environmental pollution control by the microgrid, including the environmental compensation cost of FC and MT, and the environmental compensation cost of fossil energy combustion in the distribution network. In this paper, the pollutants mainly referred to CO_2, SO_2, NO_X, and the corresponding objective functions were defined as follows:

$$C_2 = C_{fc} + C_{mt} + C_g \tag{10}$$

$$\begin{aligned} C_{fc} &= \sum_{t=1}^{T}\sum_{i=1}^{3}\alpha_j\beta_{fc,j}P_i(t)\Delta t \\ C_{mt} &= \sum_{t=1}^{T}\sum_{i=1}^{3}\alpha_j\beta_{mt,j}P_i(t)\Delta t \\ C_g &= \sum_{t=1}^{T}\sum_{i=1}^{3}\alpha_j\beta_{g,j}P_i(t)\Delta t \end{aligned} \tag{11}$$

where α_j is the unit treatment cost of pollutant j, $\beta_{mt,j}$, $\beta_{fc,j}$, $\beta_{g,j}$ are the jth pollutant emission coefficients of MT, FC, and distribution network, respectively, and $P_i(t)$ is the generating power at time t.

3.1.3. Overall objective function

The objective function of the scheduling model is to reduce the operation cost and environmental protection cost. Since the dimensions of the two objective functions were the same, to facilitate the solution, the linear weighting method was used to convert the multiple objectives into a single objective. Therefore, the overall objective function was defined as follows:

$$\min C = \omega_1 C_1 + \omega_2 C_2 \tag{12}$$

where $\omega_1 + \omega_2 = 1$, and ω_1 and ω_2 are the weights of C_1 and C_2, respectively.

3.2. System constraints

To ensure the stable and reliable operation of the microgrid, the microgrid must meet the following constraints:

Under the constraint of supply and demand balance, the generation power of the microgrid at each moment should be equal to the load demand of the microgrid.

$$P_{wt}(t) + P_{bt}(t) + P_{grid}(t) + P_{ev}(t) + P_{mt}(t) + P_{fc}(t) = P_{load}(t) \tag{13}$$

where $P_{load}(t)$, $P_{wt}(t)$, $P_{bt}(t)$, $P_{grid}(t)$, $P_{ev}(t)$, $P_{mt}(t)$ *and* $P_{fc}(t)$ is the conventional load demand, the power of WT, the power of BT, the transmission power between the distribution network and the microgrid, the power of EVs, the output of MT, and the output of FC, at time t, respectively.

The generation capacity of each dispatching unit was limited to

$$p_{i,\min} \le p_i \le p_{i,\max} \tag{14}$$

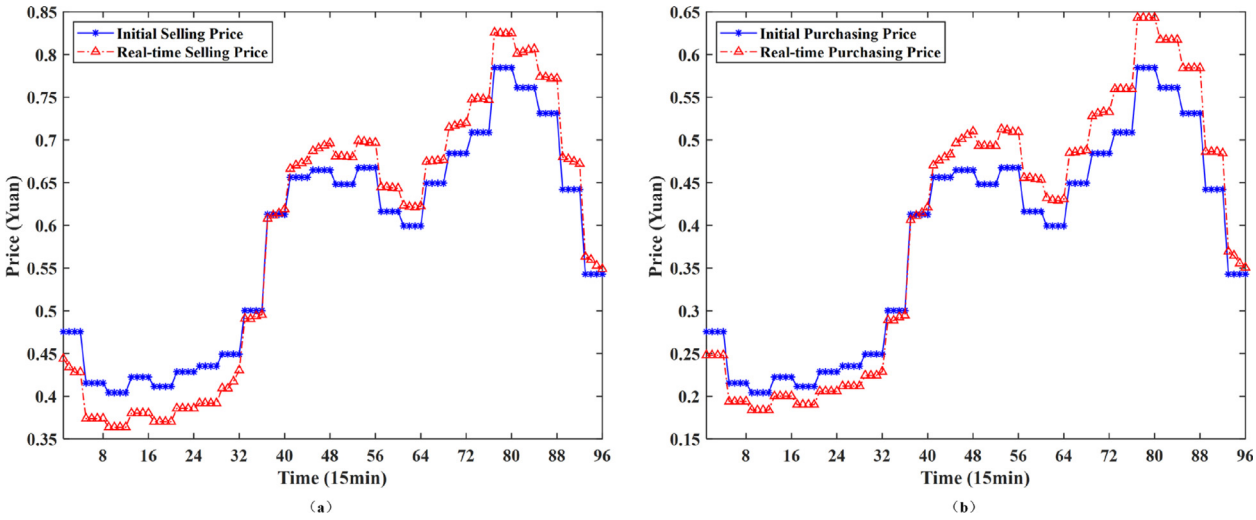

Fig. 2. Real-time electricity sale price (a) and purchase price (b).

where $p_{i,\min}$ and $p_{i,\max}$ are the upper and lower limits of the output power of the generating unit, respectively.

The constraints of energy exchange with power grid were as follows:

$$p_{grid,\min} \le p_{grid} \le p_{grid,\max} \tag{15}$$

where $p_{grid,\min}$ and $p_{grid,\max}$ are the upper and lower limits of exchange power of microgrid and distribution network, respectively.

The climbing rate r_i refers to the increase or decrease of the output power of distributed generation in unit time, which was described as follows:

$$\left|P_{i,t} - P_{i,t-1}\right| \le r_i \tag{16}$$

The charging and discharging power constraints of the battery in one hour were as follows:

$$P_{ch}^{t} \le P_{ch,\max}, P_{dis}^{t} \le P_{dis,\max} \tag{17}$$

where P_{ch}^{t} and P_{dis}^{t} are the charge and discharge power of the battery, respectively, and $P_{ch,\max}$ and $P_{dis,\max}$ are the maximum charge and discharge power of the battery, respectively.

The battery capacity constraints were described as follows:

$$SOC_j^{\min} \le SOC_j \le SOC_j^{\max} \tag{18}$$

where $SOC_j^{\max}$ and $SOC_j^{\min}$ are the upper and lower limits of the state of charge, respectively, and SOC_j is the state of charge of the battery.

3.3. Charging and discharging strategies for EVs

When EVs are in a state of disordered charging, their charging behaviour will be completely decided by the owners. The charging power curve of EVs could be simulated by using the Monte Carlo method. When the EV is disorderly connected to the microgrid, it will affect the stable operation of the microgrid as an impact load. If it is to be connected to the microgrid in an orderly manner, the economic attribute of the owner must be considered. Under the influence of real-time electricity price, the owner will want to charge when the electricity price is low, and sell electricity to the microgrid when the electricity price is high, to minimize their own costs. To optimize the charging and discharging strategy of EVs, the real-time electricity price mechanism was adopted for the microgrid.

Real-time electricity selling price, $\rho_{Sell}^{RT}(t)$ and electricity purchasing price, $\rho_{Purc}^{RT}(t)$ were expressed as follows:

$$\rho_{Sell}^{RT}(t) = \rho_{Sell}^{init}(t) \cdot \exp\{\kappa_{Sell} \frac{[P_{wt}(t) - P_{Load}^{rigid}(t)] - P_{Load}^{flex}(t)}{P_{Load}^{flex}(t)}\} \tag{19}$$

$$\rho_{Purc}^{RT}(t) = \rho_{Purc}^{init}(t) \cdot \exp\{\kappa_{Purc} \frac{[P_{wt}(t) - P_{Load}^{rigid}(t)] - P_{Load}^{flex}(t)}{P_{Load}^{flex}(t)}\} \tag{20}$$

where κ_{Sell} is the electricity selling price coefficient, κ_{Purc} is the electricity purchasing price coefficient, and $P_{wt}(t) - P_{Load}^{rigid}(t)$ is the expected flexible load of the microgrid at time t. When the flexible load is equal to the expected value, the output of renewable energy forms a balance with the load. Under this condition, the ideal working state of the system is attained where additional generation equipment is not required. $[P_{wt}(t) - P_{Load}^{rigid}(t)] - P_{Load}^{flex}(t)$ is the difference between the expected flexible load and the actual flexible load at time t. The smaller the difference, the lower the involvement of other generating equipment required.

The price of electricity was subject to rational constraints of car owners and microgrid operators:

$$\lambda_1 \rho_{Sell}^{init}(t) \le \rho_{Sell}^{RT}(t) \le \lambda_2 \rho_{Sell}^{init}(t) \tag{21}$$

$$\lambda_1 \rho_{Purc}^{init}(t) \le \rho_{Purc}^{RT}(t) \le \lambda_2 \rho_{Purc}^{init}(t) \tag{22}$$

$\lambda_1 \rho_{Sell}^{init}(t)$ is the lowest price that the microgrid operator can afford at time t, and $\lambda_2 \rho_{Sell}^{init}(t)$ is the highest price that the user can accept at time t.

By raising or lowering the price of electricity, EVs could be guided to charge and discharge in an orderly manner. Fig. 2(a) and (b) shows the real-time electricity prices.

3.4. Microgrid dispatching strategy

In the dispatching of the microgrid system, since wind turbines generate electricity from renewable energy, they do not cause environmental pollution, and their output curve could be predicted using prediction technology. Additionally, the curve of EVs could be simulated using the Monte Carlo method, such that they are given priority to meet the predicted load. Secondly, the system judges the capacity and working mode of the energy storage device, such that MT and FC are economically and environmentally scheduled and traded. To maintain the reliability of the microgrid, the microgrid is connected to the grid, and the distribution network is used as the standby capacity in the

strategy. In this paper, the scheduling direction of load, and the amount of shortage of wind turbines and EVs was divided into two directions: the supply was greater than the demand, and the supply was less than the demand. The scheduling strategy of the microgrid was determined according to the cost at every moment.

4. Optimization method

4.1. Linear weighting method based on two-person zero-sum game

Multiple targets can be solved using many methods. The linear weighting method is a typical one, which converts the multiple targets into a single target by setting different weights for each target. The objective function is converted to the following formula:

$$\begin{aligned} &\min\ f(x) = \sum_{i=1}^{n} \lambda_i f_i(x) \\ &s.t.\quad G(x) \le 0,\ H(x) \le 0 \end{aligned} \tag{23}$$

However, the disadvantage of this method is that it is difficult to determine the weight of each target, and the current methods to determine the weights has great subjectivity. Additionally, the microgrid system used in this paper contains renewable energy, which will interfere with the scheduling because of its randomness. Therefore, to avoid the interference of uncertain factors, and obtain objective weights, we used a method of weight determination based on the two-person zero-sum game.

From the perspective of game theory, there are two decision makers in the optimal dispatching of power system with renewable energy. One is the manual decision maker, and the instructions issued can realize the complete consumption of wind power; the other is nature, it will determine the output of the WT, which will affect the output of other devices in a microgrid. On this basis, nature is personified as a player to play a game with decision-makers, and then the microgrid scheduling is obtained. This scheduling is not only objective, but also reduces the interference of nature in the scheduling. Therefore, the weight determination method used in this paper was the two-person zero-sum game method.

We assumed that the original multi-objective optimization problem had n objectives: $f_1, f_2, \ldots, f_n$. When the objective i is optimized separately, the optimal solution of the original problem is recorded as x_i^*, and the set of the optimal solution is recorded as X^*. Furthermore, we assumed that there were two participants in the game, the first participant selected a strategy from f_i as its strategy, and the second participant selected a solution from the set of optimal solutions as its strategy. The typical two-person zero-sum game model is expressed as follows:

(1) Participants: Participant 1 and Participant 2 (virtual participants)

$$f_i \in \{f_1, f_2, \ldots, f_n\}$$

(2) Policy setting:

$$x_i \in \{x_1^*, x_2^*, \ldots, x_n^*\}$$

(3) Payment: $f_i(x_i)$ and $-f_i(x_i)$

Since the dimensions of each objective function in the original problem were not the same, the objective function needed to be normalized as follows:

$$f_{ij}' = \frac{f_i(x_j^*)}{f_i(x_i^*)},\ i, j = 1, 2, \ldots, n \tag{24}$$

λ_i' represents the probability that participant 1 chooses f_i as its strategy, and μ_i' be the probability that participant 2 chooses x_j^* as its strategy. The expected payment of participant 1 was expressed as follows:

$$F' = \sum_{i=1}^{n}\sum_{j=1}^{n} f_{ij}' \lambda_i' \mu_j' \tag{25}$$

If F' denotes a certain cost, then the goal of participant 1 is to minimize, and the goal of participant 2 is to maximize, that was

$$\begin{aligned} &max_{\mu'}\ min_{\lambda'} F' = max_{\lambda'}\ min_{\mu'} F' \\ &s.t.\quad \sum_{i=1}^{n} \lambda_i' = 1,\ \lambda' \ge 0 \\ &\qquad \sum_{i=1}^{n} \mu_i' = 1,\ \mu' \ge 0 \end{aligned} \tag{26}$$

The solution of the game problem was equivalent to solving the two following linear programming problems:

$$\begin{aligned} &\max \sum_{i=1}^{n} r_i \\ &s.t.\quad r_i \ge 0 \\ &\sum_{i=1}^{n} f_{ij}' r_i \le 1, j = 1, 2, \ldots, n \end{aligned} \tag{27}$$

$$\begin{aligned} &\min \sum_{j=1}^{n} s_j \\ &s.t.\quad s_j \ge 0 \\ &\sum_{j=1}^{n} f_{ij}' s_j \le 1, i = 1, 2, \ldots, n \end{aligned} \tag{28}$$

The optimal payoff obtained by solving the above two optimization problems was as follows:

$$F^* = \frac{1}{\sum r_i^*} = \frac{1}{\sum s_j^*} \tag{29}$$

The mixed strategy Nash equilibrium of the game problem was expressed as follows:

$$\lambda_i'^* = F^* r_i^*,\ \mu_j'^* = F^* s_j^* \tag{30}$$

Then, the weight coefficient of each objective of the original optimization problem was expressed as follows:

$$\lambda_i = \frac{\lambda_i'}{f_{ii} \sum_{i=1}^{n} (\lambda_i'/f_{ii})},\ i = 1, 2, \ldots, n \tag{31}$$

This weight coefficient could be introduced into the original problem, and the multi-objective problem could be transformed into a single-objective optimization problem for solution. Therefore, this method overcame the deficiency of the general weighted coefficient method relying on the subjectivity of decision-makers.

4.2. Adaptive simulated annealing particle swarm optimization

PSO is an algorithm that imitates the process of birds flying and foraging. It considers each individual as a particle that flies at a certain speed, then updates its position and speed according to experience, dynamically adjusts from the best position of the individual to the best position of the group, and finally outputs a global optimal solution (Ma et al., 2018). Since PSO is affected by inertia weight and learning factor, it can easily to fall into the local optimum. Therefore, it is often necessary to improve its inertia weight and learning factor to obtain the global optimum.

The idea of a simulated annealing (SA) algorithm originates from the cooling process of a solid. If the temperature of the solid is high, its energy will be higher, and the particles in the solid will be in a state of disordered motion. SA includes the annealing process and the Metropolis criterion. Annealing refers to the process of gradually cooling an object. The SA algorithm starts from a higher initial temperature. If the temperature gradually decreases, the solution of the algorithm will gradually tend to be stable, but the solution at this time is the local optimal solution,

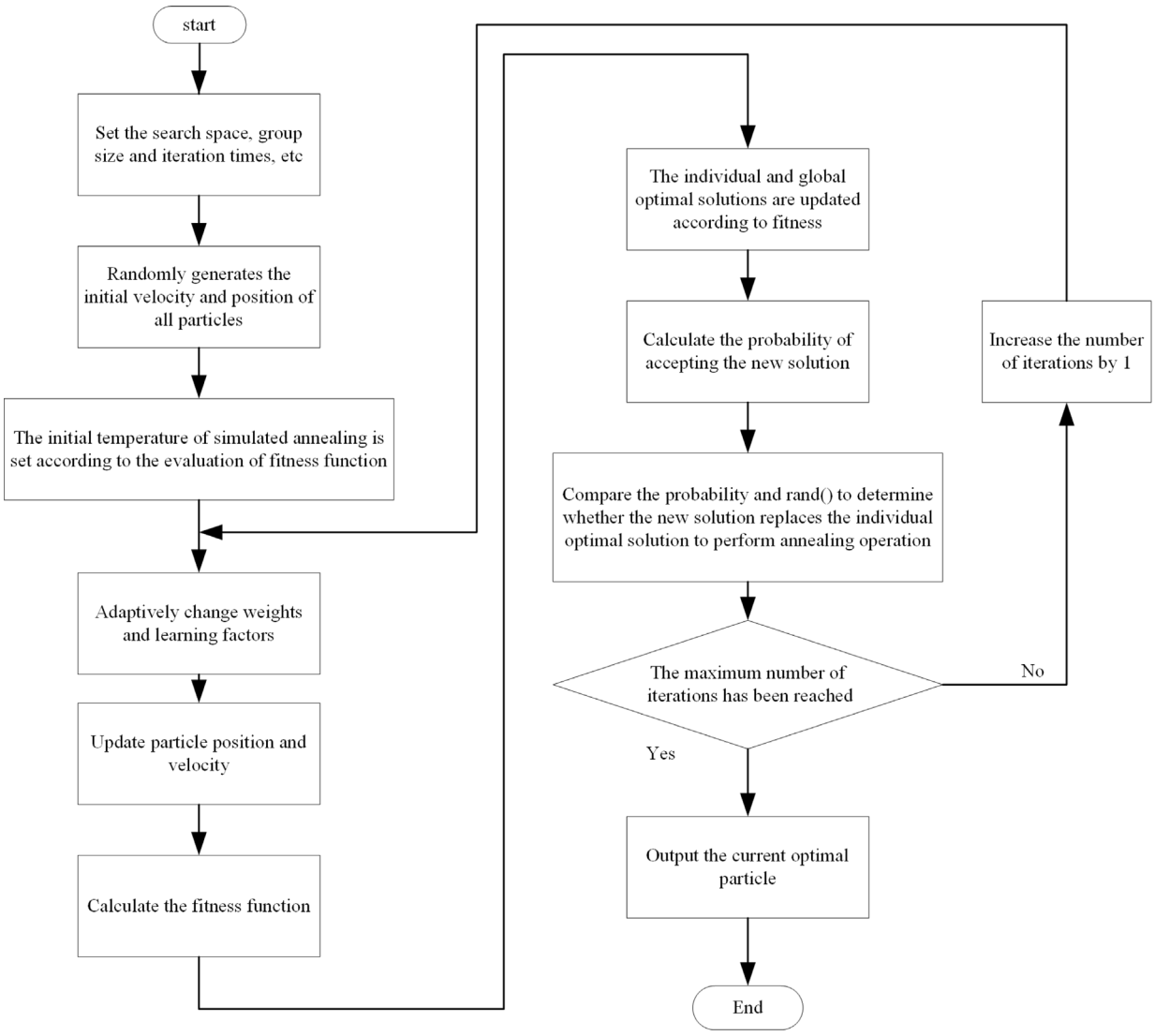

Fig. 3. Flow-chart of adaptive simulated annealing particle swarm optimization.

and the Metropolis criterion must be used to help the algorithm jump out of the local solution, and achieve the global optimal (Ge and Ak, 2021).

According to the Metropolis criterion, the SA algorithm determines whether the optimal solution of each iteration can replace the individual optimal solution, which is expressed as follows (Jza et al., 2021) :

$$p_i(k) = \begin{cases} 1 & , E_i(k) \le E(g) \\ e^{-\frac{E_i(k)-E(g)}{T_i}} & , E_i(k) > E(g) \end{cases} \tag{32}$$

where $E_i(k)$ represents the energy of the i particle in the kth iteration, it is the fitness value of the particle. $E(g)$ represents the optimal energy of the current population, and T_i represents the current temperature.

Therefore, in this paper, we used ASAPSO to optimize the scheduling results, and conducted adaptive processing on the inertia weight and learning factor of particle swarm (Zhou et al., 2021) as follows:

$$\begin{aligned} \omega = {} & (\omega_{\max} + \omega_{\min})/2 \\ & + \tanh(-4 + 8 * (k_{\max} - k)/k_{\max})(\omega_{\max} + \omega_{\min})/2 \end{aligned} \tag{33}$$

$$\begin{aligned} c_1 &= c_{1\_start} + \frac{(c_{1\_end} - c_{1\_start}) * n}{N} \\ c_2 &= c_{2\_start} + \frac{(c_{2\_end} - c_{2\_start}) * n}{N} \end{aligned} \tag{34}$$

where $\omega_{\max}$ and $\omega_{\min}$ are the maximum and minimum values of the weight coefficient, respectively. In this paper, $c_{1\_start} = 3$, $c_{1\_end} = 1$, $c_{2\_start} = 1$ and $c_{2\_end} = 3$.

The Metropolis criterion in the SA algorithm involves the change of temperature, and the initial temperature must be designed according to the fitness function. With the increase in the number of iterations, the temperature decreases with a certain cooling coefficient, and the specific expression was as follows:

$$T(k) = \begin{cases} E(P_{best})/\log(0.2), & k = 1 \\ T(k-1) * \mu & , k > 1 \end{cases} \tag{35}$$

where the cooling coefficient, $\mu = 0.95$.

After each iteration, the probability of accepting the new solution is calculated according to Eq. (32) and compared with *rand*() to determine whether to accept the new solution. Thus, the ability of the algorithm to jump out of the local optimal solution can be improved.

Fig. 3 shows the specific steps of the ASAPSO algorithm.

Table 1
Basic data of distributed generation.

Type	Lower limit of output/kW	Output ceiling /kW	Shipped to maintain several($K_{om,i}$)	Capacity factor (%)	Depreciable life (year)	Initial installation cost per unit capacity (¥/kW)
WT	0	200	0.0296	22.13	10	23 750
FC	0	60	0.0293	36.73	10	42 750
MT	0	60	0.0419	54.99	15	16 090
BT	0	40	0.0450	32.67	10	8700

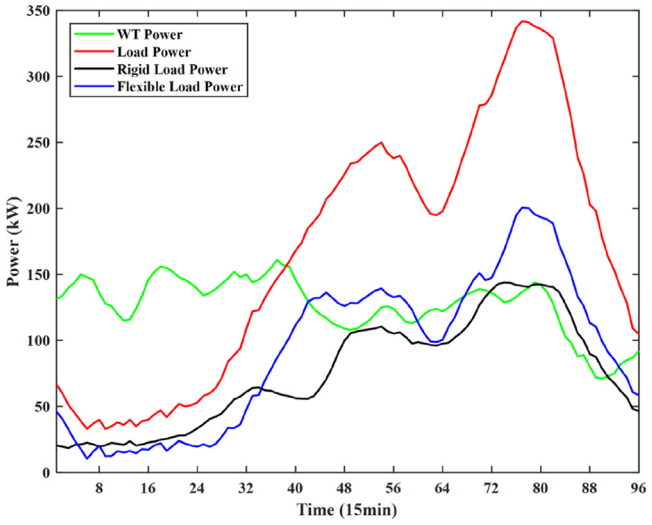

Fig. 4. Power curve.

Table 2
Discharge coefficient data of pollutant treatment.

contaminant	α_j/(¥/kg)	β_{fc}/(g/kWh)	β_{mt} (g/kWh)	β_g/(g/kWh)
CO_2	0.21	489.4	184	889
SO_2	14.842	0.003	0.001	1.8
NO_X	62.694	0.014	0.619	1.6

5. Case studies

The microgrid mainly uses wind power generation. BT, FC, MT, and EVs are auxiliary power sources, and the main grid is used as standby capacity. To improve the economy and environmental protection of the microgrid, the operation cost and environmental protection cost of the microgrid were considered, and the microgrid dispatching strategy was optimized while the uncertainty of supply and demand was considered.

5.1. Scenario design

Fig. 4 shows the wind power and load in the microgrid used in this paper. We considered different operation modes of EVs, and selected the two following scenarios. Scenario 1: EVs are in disorderly charging; Scenario 2: EVs are charged and discharged orderly under the guidance of real-time electricity price. According to the user's charging behaviour and market price, the power curve was simulated using the Monte Carlo method, and 80 EVs were selected for simulation. Fig. 5(a) and (b) show the disordered charging, and orderly charging and discharging simulated using the Monte Carlo method, and Fig. 6 shows its equivalent load curve. Table 1 lists the basic data of the microgrid distributed generation adopted in this paper, and Table 2 lists the pollutant treatment emission coefficient data. Fig. 7 shows the peak–valley electricity price traded with the distribution network.

Table 3
Zero-sum game payoff matrix.

Objective function	x^p	x^c
f_1/¥	882.3384	1057.828
f_2/¥	282.3136	101.5335

5.2. Simulation results

5.2.1. Optimization results of this paper

In this paper, we analysed scenario 2, where some EVs were in an orderly charge and discharge state. Firstly, two objective functions were transformed into a single objective function by a two-person zero-sum game, and then the scheduling strategy was optimized using ASAPSO. When the load deficiency was less than zero, the excess electricity was charged to the BT, and if there was surplus electricity, it was sold to the distribution network. When the load deficiency was greater than zero, the BT, FC, and MT could generate electricity to meet the load within the rated power, and if the load was not satisfied, power was purchased from the distribution to meet this part of the load.

First, we considered operation cost and environmental governance cost of the microgrid as the optimization objectives, used ASAPSO to optimize their objective functions to obtain the optimization results, which were recorded as x^p and x^c, respectively, and the corresponding operation cost f_1 and environmental governance cost f_2 were calculated. Then, the two virtual players were introduced, and the corresponding game strategies were f_1, f_2 and x^p, x^c; thus, a two-person zero-sum game problem was formulated. Table 3 lists the zero-sum game payoff matrix of the optimization problem.

Then, the output of each target was normalized, and the payment matrix was expressed as follows:

$$f' = \begin{bmatrix} 1 & 1.2138 \\ 2.2089 & 1 \end{bmatrix}$$

The Nash equilibrium of mixed strategy was solved.

$$\lambda_1^* = 0.8497, \lambda_2^* = 0.1503$$

Finally, the weight coefficient of each objective function in the original optimization problem was obtained.

$$\lambda_1 = 0.3981, \lambda_2 = 0.6019$$

Multi-objective weights were used in scheduling, and ASAPSO was used to optimize the scheduling strategy. Fig. 8(a) shows the scheduling diagram.

As seen from Fig. 8(a), when the supply was greater than the demand, the BT was charged, and the surplus electricity was sold to the distribution network. EVs were charged in an orderly manner under the guidance of the price of electricity, and the renewable energy from wind power was fully absorbed. Furthermore, when the supply was less than the demand, renewable energy from wind power was preferred, and the remaining load was mainly met by BT, MT, and FC. Under the guidance of electricity price, EVs underwent orderly discharge, and the distribution network served as the reserve capacity to achieve full load-bearing.

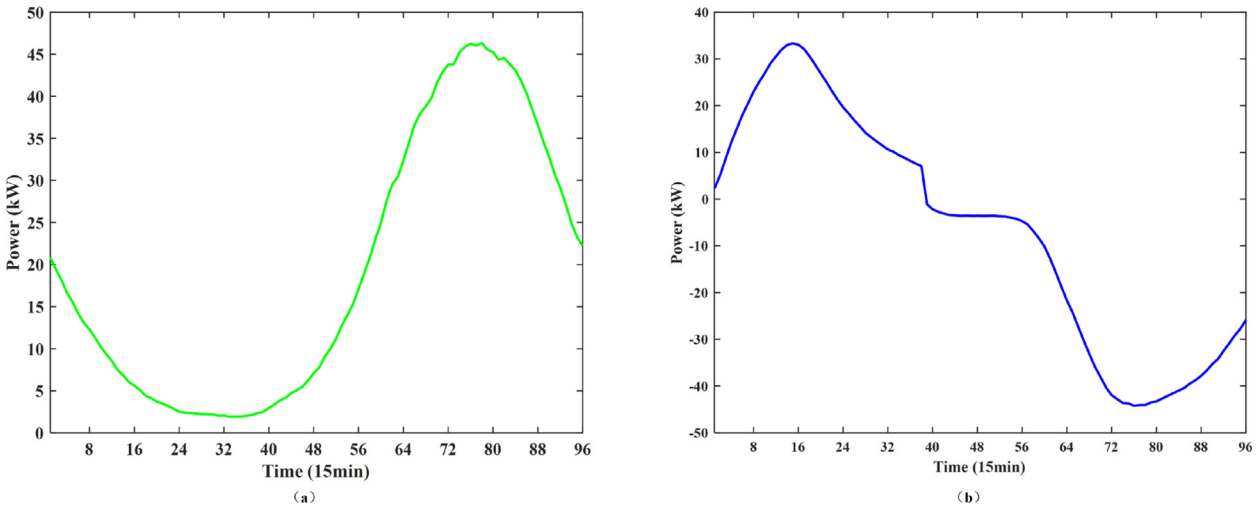

Fig. 5. Chart of disordered charging (a) and orderly charging and discharging of EVs (b).

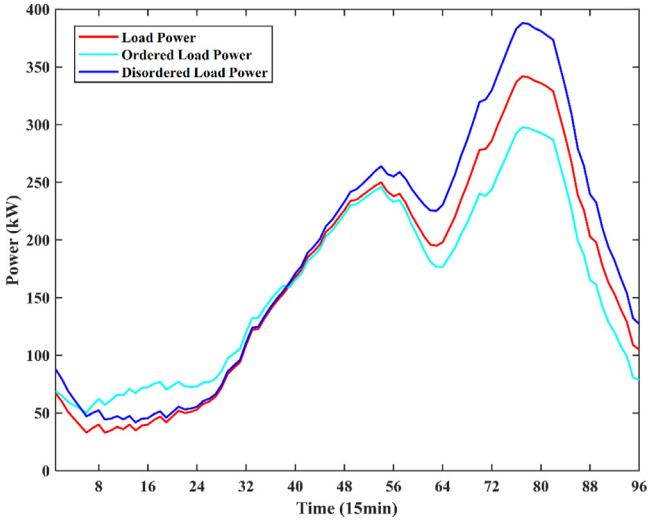

Fig. 6. Equivalent load diagram.

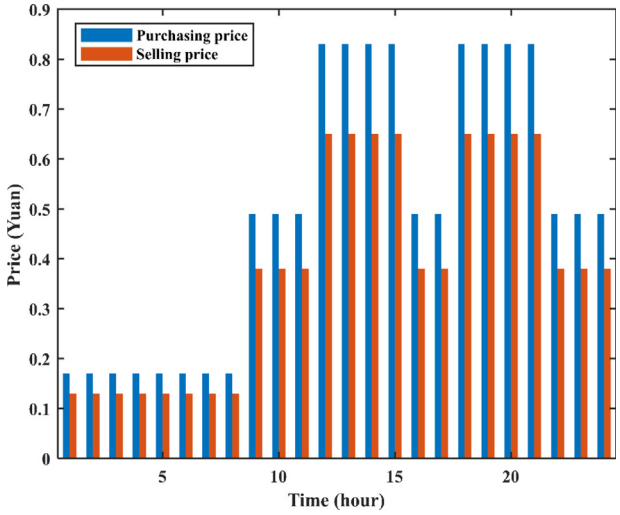

Fig. 7. Time-of use (TOU) electricity price.

5.2.2. Comparative analysis of weight optimization algorithms

To verify the performance of the weight determination method used in this paper, ASAPSO was used as the optimization algorithm, and the weights obtained in this paper were compared and analysed by using the single objective function with the best economy, the single objective function with the best environmental protection, the multi-objective function with the same weight of economy and environmental protection, the weight determined by the dualistic factor contrast method (Yang et al., 2018b), and the entropy method (Tan et al., 2016).

The dualistic factor contrast method considered the importance level of environmental protection to be "slightly" above economy. After establishing the importance qualitative ranking scale matrix and consistency test, it converted the fuzzy tone operator into the non-normalized weight vector of membership index: [0.739,1], and the normalized index weights, $\lambda_1 = 0.425$, $\lambda_2 = 0.575$. The entropy method used information entropy method to calculate the entropy value of each index, and got the weights according to the entropy value. When the value difference of an index is large, the entropy value is small, indicating that the effective information provided by the index is large, and its corresponding weight is also large. In the experiment, there were two indicators: operating cost and environmental maintenance cost. We took six groups of economic costs and environmental protection costs to form a matrix, used these data to calculate the entropy weight, and further obtained the weights as follows: $\lambda_1 = 0.375$, $\lambda_2 = 0.625$.

Fig. 8(b), (c), (d), (e) and (f) respectively show the scheduling curves of the microgrid with the best economic performance, the best environmental protection, the same weight of economic and environmental protection, the dualistic factor contrast method, and the entropy method. Table 4 lists the scheduling results under different weights.

Fig. 8(b) shows that when supply exceeded demand, the scheduling curve trend was consistent with that shown in Fig. 8(a). In the case of short supply, the BT, MT, FC, and distribution network jointly met the shortage load. Since the best economic state was to reduce the operation cost of the system as much as possible under the condition of ensuring the power demand, and the power purchase cost of the distribution network was lower than that of MT and FC, it was necessary to purchase power from the distribution network as much as possible during dispatching. It is seen from Fig. 8(c) that when the supply exceeded the demand, the scheduling curve trend was consistent with that

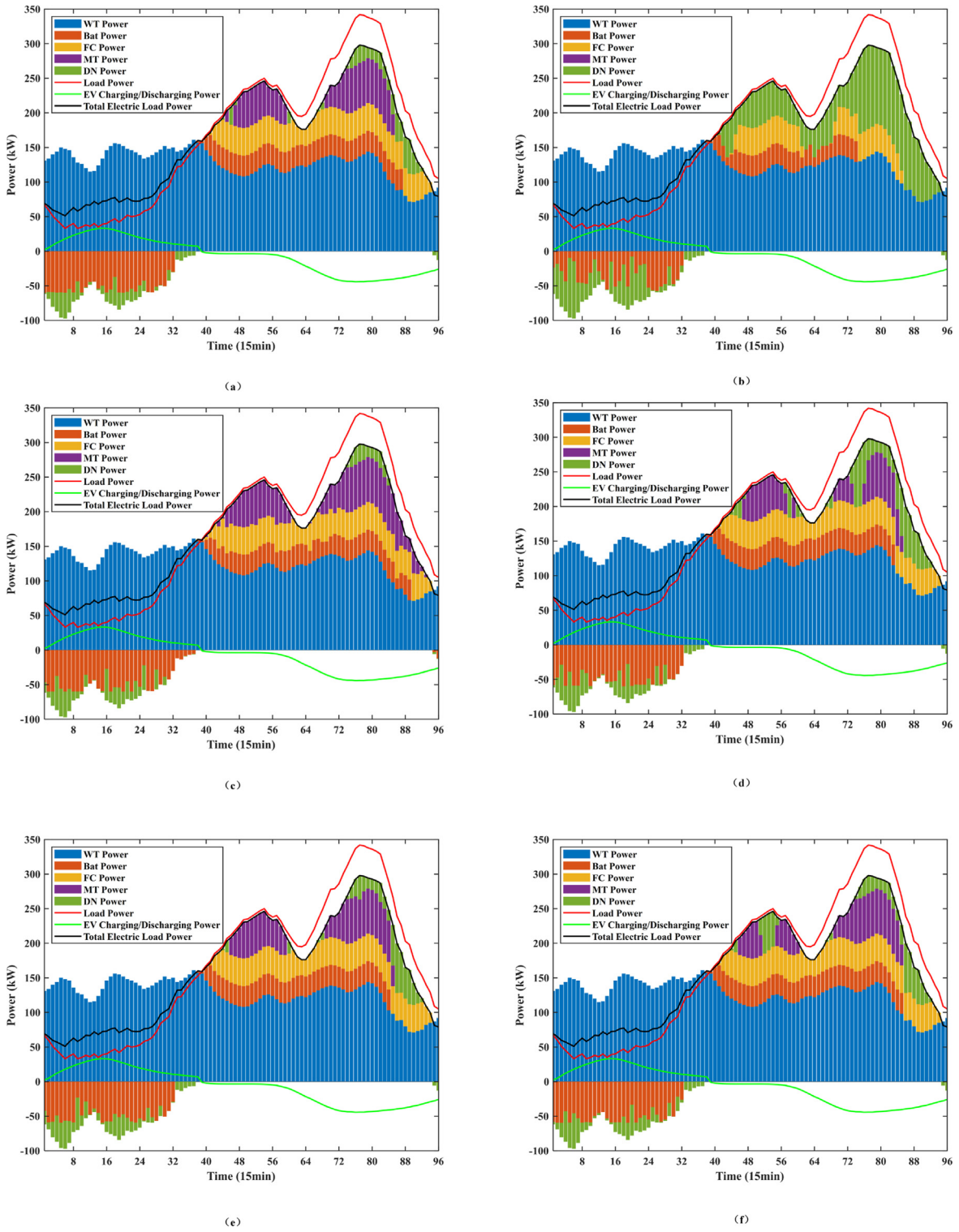

Fig. 8. (a) Scheduling results under the two-person zero-sum game method, (b) Scheduling results under economy, (c) Scheduling results under environmental protection, (d) Scheduling results under environmental protection and environmental protection, (e) Scheduling results under the dualistic factor contrast method, (f) Scheduling results under the entropy method.

shown in Fig. 8(a). When the supply was less than the demand, the BT, MT, FC, and distribution network met the shortage load, and the best state of environmental protection was to reduce the environmental maintenance cost of microgrid. Due to the high pollution gas treatment cost of the distribution network, BT, FC and MT were used to meet the load, and the distribution network was used as standby capacity. It is seen from Fig. 8(d), (e) and (f) that the trend of dispatching curves were consistent with that shown in Fig. 8(a).

Table 4 lists the data of six experiments. When the economy was considered, the average operating cost was the lowest and average environmental protection cost was the highest; When the environmental protection was considered, its average environmental protection cost was the lowest, the average operation

Table 4
The costs for different weights.

Method	Weight	Average operating cost/¥	Average environmental cost/¥	Total cost/¥
Extremum method	(1,0)	883	286	1169
Equal weight	(0.5,0.5)	985	151	1136
Extremum method	(0,1)	1063	102	1165
Dualistic factor contrast method	(0.425,0.575)	994	137	1131
Entropy method	(0.375,0.625)	1005	124	1129
Two-person zero-sum game method	(0.3981,0.6019)	1001	122	1123

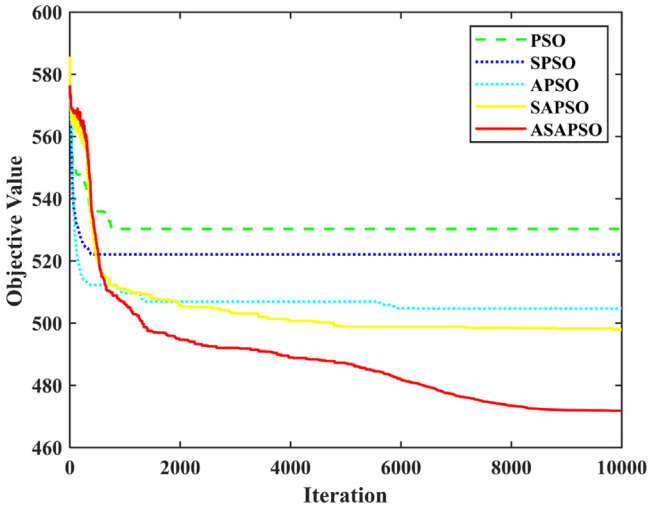

Fig. 9. Performance comparison of the algorithms.

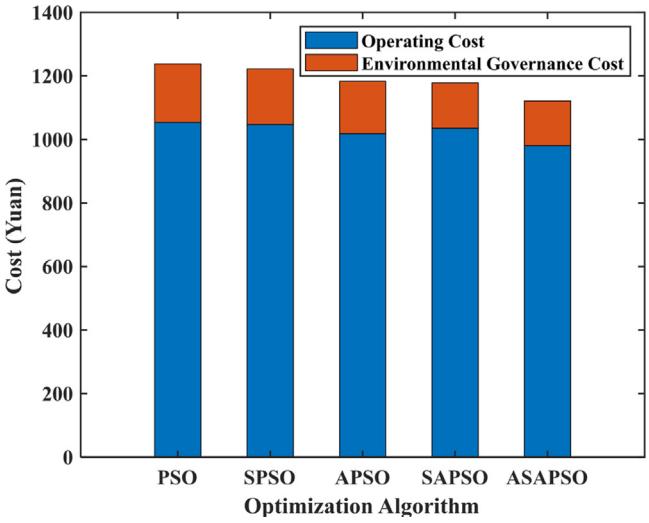

Fig. 10. Cost diagram of the optimization algorithm.

cost was the highest; When the economy and environmental protection were considered equally important, and the weights were obtained from the dualistic factor contrast method and the entropy method, the average operating cost and average environmental protection cost were midway in between the values obtained while considering the economy and environmental protection separately, and the total cost was lower. When the weight was determined using a two-person zero-sum game, the average operation cost and average environmental protection cost were close to that when the weight was equal, the dualistic factor contrast method, and the entropy method; however, the total cost was lesser, which indicated that the weight determination method was more objective, and it reduced the interference of uncertain factors in the system.

5.2.3. Comparison of optimization algorithms

To validate the performance of ASAPSO, PSO, standard PSO (SPSO), adaptive PSO (APSO), and simulated annealing PSO (SAPSO) were compared and analysed in the experiment. The five algorithms were maintained consistent in certain parameter settings to obtain accurate comparison results. To prove the effectiveness of the algorithm, six experiments were carried out, and the comparison of the fitness values of the six experiments is shown in Fig. 10, Fig. 11 shows the scheduling cost of each algorithm, Fig. 12 shows the state of charge (SOC) curve of the BT of five algorithms, and Table 5 lists the average and standard deviation of the fitness values and total cost of the six experiments.

It is seen from Fig. 9 that there was no essential difference between the different algorithms in the initial stage; however, the convergence speed of each algorithm varied with the increase in the number of iterations. The order in which the different algorithms obtained the optimal results was: SPSO, PSO, APSO, SAPSO and ASAPSO; and the order of their convergence of fitness values from high to low was: PSO, SPSO, APSO, SAPSO and ASAPSO. From the convergence speed and objective value, it was seen that the convergence speed of ASAPSO was slow, but the objective value was lower than those of the other algorithms. This implied that the other algorithms fell into a local optimal state. Hence, ASAPSO could jump out of the local optimal solution, and had better global search ability. As seen from Fig. 10, the cost of APSO was lower than that of SPSO, and the cost of SPSO was lower than that of PSO, which implied that the improvement of the weight factor and learning factor in particle swarm could improve the ability of the algorithm to find the global optimum. Additionally, the cost of SAPSO was lower than that of the PSO algorithm, which indicated that SA could improve the ability of the PSO algorithm to jump out of the local optimum. Furthermore, the cost of ASAPSO was lower than that of APSO and SAPSO, which indicated that the ASAPSO algorithm had higher global search ability, and could obtain the global optimal value.

As seen from Table 5, the average value and standard deviation of the fitness value and the total cost of ASAPSO was the lowest, which implied that its optimization performance and stability performance were better, and thus, could make the dispatching results more stable, economic, and environmental friendly. Fig. 11 shows the SOC of the BT in the scheduling of the five algorithms. BT was charged before 8 a.m. and then discharged. When ASAPSO optimized the objective function, the stored power of the BT was higher than that from the other algorithms, which showed that under the scheduling of this optimization algorithm, the stored power of the BT could be better utilized, and the role of the BT can be brought into greater play. Therefore, the ASAPSO algorithm employed in this paper was superior to the general PSO algorithm.

5.2.4. Scene output analysis

Fig. 12 shows the scheduling curve of Scenario 1 where EVs were in a state of disorder, and were added to the microgrid as

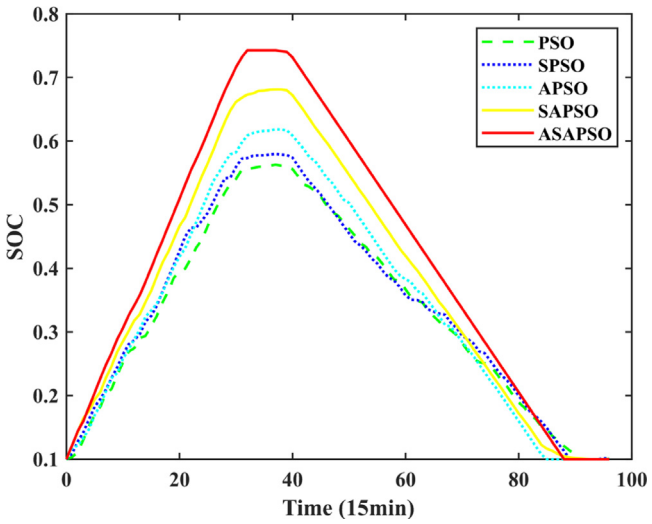

Fig. 11. SOC of BT for five algorithms.

Table 5
The average and standard deviation of objective value and total cost.

Optimization algorithm	Average of objective value	Standard deviation of objective value	Average of total cost	Standard deviation of total cost
PSO	1241	7.81	531	3.9
SPSO	1228	5.48	525	2.97
APSO	1188	4.54	505	2.21
SAPSO	1161	7.74	494	2.67
ASAPSO	1123	2.80	472	1.26

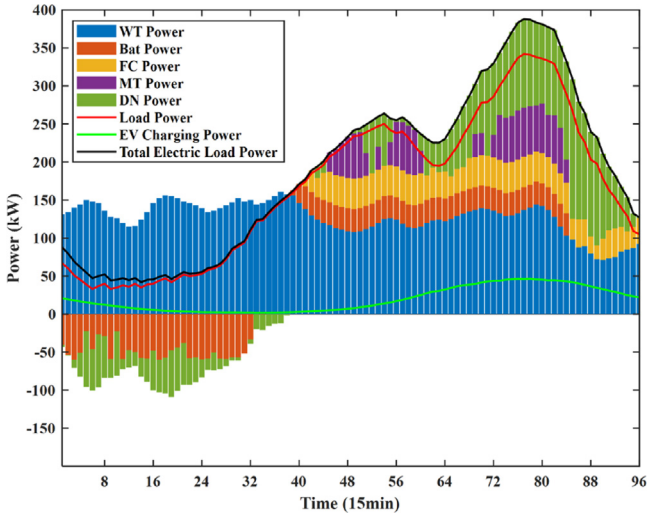

Fig. 12. Scheduling curve of scenario 1.

Table 6
Cost comparison table of Scenario 1 and Scenario 2.

	Operation cost/¥	Environmental cost/¥
Scenario 1 (EV disorder)	1180	362
Scenario 2 (EV order)	1012	125

an impact load. Its comparison with the cost of orderly charging and discharging of EVs in Scenario 2 is shown in Table 6.

As seen from Fig. 12, when the EVs were disorderly connected to the microgrid, they were regarded as load, which led to the phenomenon of adding a peak to the load peak. Compared with Fig. 8(a), when the supply was less than the demand, due to orderly access, EVs could charge when the electricity price was low, and effectively absorb renewable energy. However, when EVs were disorderly accessed, owners rarely chose to charge at that time, and thus, the charging amount of EVs was small. When the supply exceeded the demand, the EV was connected orderly, and was used as the supply side to meet part of the load in the microgrid. When the EV was connected disorderly, it was used as an impact load, which affected the stable operation in the microgrid. It is seen from Figs. 8(a) and 12, the biggest difference between scenario 1 and Scenario 2 is the power purchased from the distribution network, the orderly access of EVs could cut the peak and fill the valley in scenario 2, while the EVs added a peak on load peak in scenario 1. As shown in Table 6, scenario 2 greatly increased the power purchase from the distribution network compared with scenario 1, therefore, the operation cost and environmental maintenance cost were reduced.

6. Conclusions

In this paper, the operation characteristics of distributed generation were considered. According to the economic scheduling and energy-saving needs of a microgrid, EVs were added, and orderly charged and discharged. To reduce the influence of uncertain factors, the linear weighting method based on the two-person zero-sum game was adopted to determine the weights of the two targets, and the ASAPSO algorithm was used to solve the optimal scheduling problem of the microgrid. Furthermore, the orderly charging and discharging of EVs based on the real-time electricity price could effectively reduce the cost of microgrid and environmental governance, compared with the disorderly charging and discharging of EVs. Moreover, the linear weighting method of the two-person zero-sum game model used could obtain a relatively objective weight coefficient in this paper, which reduced the uncertainty factors in the microgrid. The ASAPSO algorithm could jump out of the local optimum and obtain the global optimum. Therefore, for the microgrid system constructed in this paper, the optimization algorithm effectively improved the economy and environmental protection of the microgrid.

CRediT authorship contribution statement

Yu Mei: Conceptualization, Methodology, Simulation, Experiment, Data analysis, Investigation, Writing – original draft & editing, Writing – review & editing. **Bin Li:** Conceptualization, Methodology, Simulation, Experiment, Data analysis, Investigation, Writing – original draft & editing, Writing – review & editing. **Honglei Wang:** Conceptualization, Methodology, Supervision, Funding acquisition, Constructive discussions, Writing – review & editing. **Xiaolin Wang:** Methodology, Supervision, Visualization, Writing – review & editing. **Michael Negnevitsky:** Methodology, Supervision, Visualization, Writing – review & editing.

Declaration of competing interest

The authors declare that they have no known competing financial interests or personal relationships that could have appeared to influence the work reported in this paper.

Acknowledgements

This work is supported by the National Natural Science Foundation of China under Grant 52067004 and the Science and Technology Plan Project of Guizhou Province under Grant [2016]5103.

References

Alomoush, M.I., 2019. Microgrid combined power-heat economic-emission dispatch considering stochastic renewable energy resources, power purchase and emission tax. Energy Convers. Manage. 200, 112090. http://dx.doi.org/10.1016/j.enconman.2019.112090.

Chamandoust, H., Bahramara, S., Derakhshan, G., 2020. Multi-objective operation of smart stand-alone microgrid with the optimal performance of customers to improve economic and technical indices. J. Energy Storage 31, http://dx.doi.org/10.1016/j.est.2020.101738.

Chen, W., Zhang, J., Lin, Y., Chen, N., Zhan, Z., Chung, H.S., Li, Y., Shi, Y., 2013. Particle swarm optimization with an aging leader and challengers. IEEE Trans. Evol. Comput. 17 (2), 241–258. http://dx.doi.org/10.1109/TEVC.2011.2173577.

Ding, X., Sun, W., Harrison, G.P., Lv, X., Weng, Y., 2020. Multi-objective optimization for an integrated renewable, power-to-gas and solid oxide fuel cell/gas turbine hybrid system in microgrid. Energy 213, 118804. http://dx.doi.org/10.1016/j.energy.2020.118804.

Ebrahim, M.A., Fattah, R., Saied, E., Maksoud, S., Khashab, H.E., 2020. Real-time implementation of self-adaptive salp swarm optimization-based microgrid droop control. IEEE Access 8, 185738-185751. http://dx.doi.org/10.1109/ACCESS.2020.3030160.

Elattar, E.E., 2018. Modified harmony search algorithm for combined economic emission dispatch of microgrid incorporating renewable sources. Energy 159 (sep.15), 496–507. http://dx.doi.org/10.1016/j.energy.2018.06.137.

Ge, A., Ak, B., 2021. Optimization of thermodynamic performance with simulated annealing algorithm: A geothermal power plant. Renew. Energy http://dx.doi.org/10.1016/j.renene.2021.03.101.

Geng, S., Wu, G., Tan, C., Niu, D., Guo, X., 2021. Multi-objective optimization of a microgrid considering the uncertainty of supply and demand. Sustainability 13 (3), 1320, https://www.mdpi.com/2071-1050/13/3/1320/pdf.

He, L., Lu, Z., Pan, L., Zhao, H., Li, X., Zhang, J., 2019. Optimal economic and emission dispatch of a microgrid with a combined heat and power system. Energies 12 (4), https://www.mdpi.com/1996-1073/12/4/604/pdf.

Huang, S., Liu, H., Wu, L., Zhou, F., Miao, W., Li, Y., Gao, J., 2019. Economic optimisation of microgrid based on improved quantum genetic algorithm. J. Eng. http://dx.doi.org/10.1049/joe.2018.8849.

Hui, H.A., Mx, A., Yan, X.B., Zx, C., Xd, A., Tao, X.A., Peng, L.A., Rc, A., 2020. Multi-objective economic dispatch of a microgrid considering electric vehicle and transferable load - ScienceDirect. Appl. Energy 262, http://dx.doi.org/10.1016/j.apenergy.2020.114489.

Javidsharifi, M., Niknam, T., Aghaei, J., Mokryani, G., 2018. Multi-objective short-term scheduling of a renewable-based microgrid in the presence of tidal resources and storage devices. Appl. Energy 216 (APR.15), 367–381. http://dx.doi.org/10.1016/j.apenergy.2017.12.119.

Jeong, Y.W., Park, J.B., Jang, S.H., Lee, K.Y., 2010. A new quantum-inspired binary PSO: Application to unit commitment problems for power systems. IEEE Trans. Power Syst. 25 (3), 1486–1495. http://dx.doi.org/10.1109/TPWRS.2010.2042472.

Jiang, H., Ning, S., Ge, Q., 2019. Multi-objective optimal dispatching of microgrid with large-scale electric vehicles. IEEE Access PP (99), 1. http://dx.doi.org/10.1109/ACCESS.2019.2945597.

Jza, B., Zl, A., Bw, A., 2021. Within-day rolling optimal scheduling problem for active distribution networks by multi-objective evolutionary algorithm based on decomposition integrating with thought of simulated annealing. Energy http://dx.doi.org/10.1016/j.energy.2021.120027.

Li, Z., Ma, J., Yu, S., Wang, H., 2015. Study on the method and application of revising the weight coefficient of three times throughout the process of evaluation. J. Comput. Methods Sci. Eng. 15 (3), 585–591. http://dx.doi.org/10.3233/JCM-150570.

Li, X., Xia, R., 2019. A dynamic multi-constraints handling strategy for multi-objective energy management of microgrid based on MOEA. IEEE Access PP (99), 1. http://dx.doi.org/10.1109/ACCESS.2019.2943201.

Liu, Lin, Bai, Ma, Chen, 2019. Multi-objective optimal scheduling method for a grid-connected redundant residential microgrid. Processes 7 (5), 296. http://dx.doi.org/10.3390/pr7050296.

Lu, X., Zhou, K., Yang, S., 2017. Multi-objective optimal dispatch of microgrid containing electric vehicles. J. Cleaner Prod. 165 (nov.1), 1572–1581. http://dx.doi.org/10.1016/j.jclepro.2017.07.221.

Lu, X., Zhou, K., Yang, S., Liu, H., 2018. Multi-objective optimal load dispatch of microgrid with stochastic access of electric vehicles. J. Cleaner Prod. http://dx.doi.org/10.1016/j.jclepro.2018.05.190, S0959652618315361.

Ma, Z., Dong, Y., Liu, H., Shao, X., Chao, W., 2018. Method of forecasting non-equal interval track irregularity based on improved grey model and PSO-SVM. IEEE Access PP, 1. http://dx.doi.org/10.1109/ACCESS.2018.2841411.

Mehrabadi, E.S., Sathiakumar, S., 2020. Multi-objective optimization of combined heat and power industrial microgrid. J. Solar Energy Eng. 142 (5), 1–15. http://dx.doi.org/10.1115/1.4046390.

Meng, X., Wang, Y., Li, C., Wang, X., Maolong, L., 2018a. Approach for uncertain multi-objective programming problems with correlated objective functions under CEV criterion. J. Syst. Eng. Electron. http://dx.doi.org/10.21629/JSEE.2018.06.08.

Meng, Y., Zhao, S., Jiang, J., 2018b. Research on multi-objective optimization operation of microgrid. IOP Conf. Ser.: Earth Environ. Sci. 189 (5), http://dx.doi.org/10.1088/1755-1315/168/1/012008.

Monteiro, J.R., Rodrigues, Y.R., Monteiro, M.R., Souza, A., Fuly, B., 2020. Intelligent RMPS allocation for microgrids support during scheduled islanded operation. IEEE Access PP (99), 1. http://dx.doi.org/10.1109/ACCESS.2020.3005081.

Moradi, M.H., Eskandari, M., Hosseinian, S.M., 2015. Operational strategy optimization in an optimal sized smart microgrid. IEEE Trans. Smart Grid 6 (3), 1. http://dx.doi.org/10.1109/TSG.2014.2349795.

Sedighizadeh, M., Fazlhashemi, S.S., Javadi, H., Taghvaei, M., 2020. Multi-objective day-ahead energy management of a microgrid considering responsive loads and uncertainty of the electric vehicles. J. Cleaner Prod. 267, 121562. http://dx.doi.org/10.1016/j.jclepro.2020.121562.

Shayeghi, H., Shahryari, E., 2017. Optimal operation management of grid-connected microgrid using multi-objective group search optimization algorithm. http://dx.doi.org/10.22098/joape.2017.3659.1290.

Tabar, V.S., Jirdehi, M.A., Hemmati, R., 2017. Energy management in microgrid based on the multi objective stochastic programming incorporating portable renewable energy resource as demand response option. Energy 118 (JAN.1), 827–839. http://dx.doi.org/10.1016/j.energy.2016.10.113.

Tan, Y., Lu, Z., Li, J., 2016. Multi-objective optimal sizing method for distributed power of wind-solar-diesel-battery independent microgrid based on improved electromagnetism-like mechanism. Power System Prot. Control 44 (8), 8, https://kns.cnki.net/kcms/detail/detail.aspx?dbcode=CJFD&dbname=CJFDLAST2016&filename=JDQW201608010&uniplatform=NZKPT&v=Hmahkukp-qRyHvK2O5iQRaVCZFRuVonH_TYbGuvuoZR9B6Z8R07J2FCUwFMUa02A.

Vivek, Mohan, Jai, Govind Singh, Weerakorn, Ongsakul, 2017. Sortino ratio based portfolio optimization considering EVs and renewable energy in microgrid power market. IEEE Trans. Sustain. Energy http://dx.doi.org/10.1109/PESGM.2017.8274115.

Wang, Y., Lu, Y., Ju, L., Wang, T., Tan, Q., Wang, J., Tan, Z., 2019. A multi-objective scheduling optimization model for hybrid energy system connected with wind-photovoltaic-conventional gas turbines, CHP considering heating storage mechanism. Energies 12 (3), http://dx.doi.org/10.3390/en12030425.

Xu, Z., Yang, P., Wen, J., 2016. Multi-objective optimization of microgrid with hybrid energy storage system. Mod. Electr. Power 33 (02), 5–9, https://kns.cnki.net/kcms/detail/detail.aspx?dbcode=CJFD&dbname=CJFDLAST2016&filename=XDDL201602001&uniplatform=NZKPT&v=UL_gdo65ZUjlc7HRMfNXF2z80aZVx63H2TEvuGjk8yeaSw41oY2l5lKURC2tOUEJ.

Xue, H., Bai, Y., Hu, H., Xu, T., Liang, H., 2019. A novel hybrid model based on TVIW-PSO-GSA algorithm and support vector machine for classification problems. IEEE Access 1. http://dx.doi.org/10.1109/ACCESS.2019.2897644.

Yang, X., Long, J., Liu, P., Zhang, X., Liu, X., 2018a. Optimal scheduling of microgrid with distributed power based on water cycle algorithm. Energies 11 (9), 2381. http://dx.doi.org/10.3390/en11092381.

Yang, W., Ma, X., Xu, M., Bian, X., 2018b. Research on scheduling optimization of grid-connected micro-grid based on improved brid swarm algorithm. Adv. Technol. Electr. Eng. Energy 37 (2), 8, https://kns.cnki.net/kcms/detail/detail.aspx?dbcode=CJFD&dbname=CJFDLAST2018&filename=DGDN201802007&uniplatform=NZKPT&v=wEktVxa8jZo4evhkYaqV9MQBIBo55vXcfBoeo7uhuAz-WLKSNavwEvFFn_iN3TXJ.

Yu, Y., Liang, R., Liu, J., Xu, Y., 2019. Optimal scheduling of power system based on zero-sum game. China Sciencepap. 14 (05), 548–552, https://kns.cnki.net/kcms/detail/detail.aspx?dbcode=CJFD&dbname=CJFDLAST2019&filename=ZKZX201905013&uniplatform=NZKPT&v=hvdn7xC2YHPqY7UJ1uemMXepzqu_4xif8iBquoO_YU4gRQCai8McrwyfLchC0Mri.

Zhao, Y., Xu, T., Li, Y., Cui, L., Chen, X., 2020a. Research on electric vehicle scheduling strategy based on time-shared electricity price. Power Syst. Prot. Control 48 (11), 10, https://kns.cnki.net/kcms/detail/detail.aspx?dbcode=CJFD&dbname=CJFDLAST2020&filename=JDQW202011012&uniplatform=NZKPT&v=dCzJj4Mz2gtLLjjmhR1el4cMstjP_XlBUGP-CN1-A6-AFGnGWDun2G_awm1wiS91.

Zhao, X.G., Zhang, Z.Q., Xie, Y.M., Meng, J., 2020b. Economic-environmental dispatch of microgrid based on improved quantum particle swarm optimization. Energy 195 (Mar.15), 117014.117011-117014.117015. http://dx.doi.org/10.1016/j.energy.2020.117014.

Zheng, J.H., Wu, C.Q., Huang, J., Liu, Y., Wu, Q.H., 2020. Multi-objective optimization for coordinated day-ahead scheduling problem of integrated electricity-natural gas system with microgrid. IEEE Access PP (99), 1. http://dx.doi.org/10.1109/ACCESS.2020.2993263.

Zhou, S., Liu, X., Hua, Y., Zhou, X., Yang, S., 2021. Adaptive model parameter identification for lithium-ion batteries based on improved coupling hybrid adaptive particle swarm optimization- simulated annealing method. J. Power Sources 482, 228951. http://dx.doi.org/10.1016/j.jpowsour.2020.228951.